© 2014. Published by The Company of Biologists Ltd | Journal of Cell Science (2014) 127, 4260–4269 doi:10.1242/jcs.153239

RESEARCH ARTICLE

Progressive quality control of secretory proteins in the early secretory compartment by ERp44

Sara Sannino[1,2], Tiziana Anelli[1,3], Margherita Cortini[1,*], Shoji Masui[4], Massimo Degano[1,3], Claudio Fagioli[1,3], Kenji Inaba[4] and Roberto Sitia[1,3,‡]

ABSTRACT

ERp44 is a pH-regulated chaperone of the secretory pathway. In the acidic milieu of the Golgi, its C-terminal tail changes conformation, simultaneously exposing the substrate-binding site for cargo capture and the RDEL motif for ER retrieval through interactions with cognate receptors. Protonation of cysteine 29 in the active site allows tail movements *in vitro* and *in vivo*. Here, we show that conserved histidine residues in the C-terminal tail also regulate ERp44 *in vivo*. Mutants lacking these histidine residues retain substrates more efficiently. Surprisingly, they are also O-glycosylated and partially secreted. Co-expression of client proteins prevents secretion of the histidine mutants, forcing tail opening and RDEL accessibility. Client-induced RDEL exposure allows retrieval of proteins from distinct stations along the secretory pathway, as indicated by the changes in O-glycosylation patterns upon overexpression of different partners. The ensuing gradients might help to optimize folding and assembly of different cargoes. Endogenous ERp44 is O-glycosylated and secreted by human primary endometrial cells, suggesting possible pathophysiological roles of these processes.

KEY WORDS: ERp44, Golgi, O-glycosylation, Endoplasmic reticulum, Protein quality control, Protein secretion

INTRODUCTION

ERp44 is a multifunctional chaperone of the PDI-family that regulates Ca^{2+} signaling, redox homeostasis and thiol-dependent protein quality control at the endoplasmic reticulum (ER)–Golgi interface (Anelli et al., 2012; Cortini and Sitia, 2010). ERp44 is key for the retrieval of orphan subunits of disulfide-linked oligomers, like IgM and adiponectin (Anelli et al., 2003; Anelli et al., 2007; Qiang et al., 2007; Wang et al., 2007) and for the intracellular localization of Ero1 oxidases, Sumf1 and peroxiredoxin 4 (Prx4) (Fraldi et al., 2008; Kakihana et al., 2013; Otsu et al., 2006). It associates with its client proteins covalently through cysteine 29 (C29) and non-covalently, likely through the surrounding hydrophobic patches in the substrate-binding site (SBS). In the available crystal structure, the SBS is shielded by a C-terminal tail (C-tail) (Wang et al., 2008). Tail movements simultaneously expose the SBS and the C-terminal RDEL, allowing interaction with the KDEL receptors (KDELR) and, hence, the retrieval to the ER of the chaperone and its client proteins (Anelli et al., 2003; Cortini and Sitia, 2010; Vavassori et al., 2013).

We demonstrated recently that the pH gradient existing along the early secretory compartment (ESC), a term used herein to define the ER, ER–Golgi intermediate compartment (ERGIC) and Golgi complex, regulates C29 protonation and, consequently, ERp44 tail opening (Vavassori et al., 2013). In the closed state, C29 is concealed in the interface between domain-a and the C-tail, forming the hydrogen bonds with the side chains of T369 and S32 and the main chain amides of F31 and S32. At lower pH, however, the hydrogen bonds are significantly weakened, probably due to the protonation of the C29 thiol group, leading to the release of the C-tail. Such pH-dependent conformational change is advantageous in the regulated Golgi to ER transport of client proteins by ERp44. Besides C29, T369 and S32, we also noted that five histidine residues located at the border between the domain-b′ and the C-tail are highly conserved in the ERp44 family proteins (Fig. 1A). To test the possibility that these residues could also contribute in modulating ERp44 activity, we here generated deletion and replacement mutants and analyzed their activity *in vitro* and *in vivo*. Our data reveal a new mechanism controlling the binding of both clients and KDELR by ERp44 at ER–Golgi interface. We also show that O-glycosylated ERp44 can be secreted by certain cell types.

RESULTS

In the available ERp44 crystals, part of the C-tail (residues 332–350) is not resolved due to the lack of electron density (Wang et al., 2008). Two histidine residues at the beginning of this unstructured fragment (332–333) and additional ones in the upstream helices (299, 323 and 328) are highly conserved in ERp44 (Fig. 1A), as are the surrounding sequences. To investigate the potential regulatory role of this histidine-rich region, we first replaced residues 326–350 with a short spacer (SGSG) to generate the ΔHis mutant (see supplementary material Fig. S1A for details) and investigated its *in vitro* reactivity with maleimide modified with polyethylene glycol 2000 (MalPEG) (Fig. 1B) or 1-anilinonaphthalene-8-sulfonate (ANS) (Fig. 1C) as a function of pH. ERp44 contains two unpaired cysteine residues (C29 and C63) and four cysteine residues engaged in structural disulfide bonds (C160–C212 and C272–C289 in domains b and b′, respectively) (Wang et al., 2008). In a preceding study, we found that C29 was the primary residue that reacts with MalPEG, whereas C63 was also modifiable, although with much lower

[1]Divisions of Genetics and Cell Biology and Immunology, Transplantation and Infectious Diseases, IRCCS Ospedale San Raffaele, 20132 Milan, Italy. [2]Department of Bioscience, Università degli Studi di Milano, Via Celoria 26, 20133 Milan, Italy. [3]Università Vita-Salute San Raffaele, 20132 Milan, Italy. [4]Institute of Multidisciplinary Research for Advanced Materials, Tohoku University Katahira 2-1-1, Aoba-ku, Sendai 980-8577, Japan.
*Present address: Department of Life Science, Università of Modena and Reggio Emilia, 41125 Modena, Italy.

‡Author for correspondence (r.sitia@hsr.it)

Received 18 March 2014; Accepted 17 July 2014

Journal of Cell Science

Journal of Cell Science (2014) 127, 4260–4269 doi:10.1242/jcs.153239

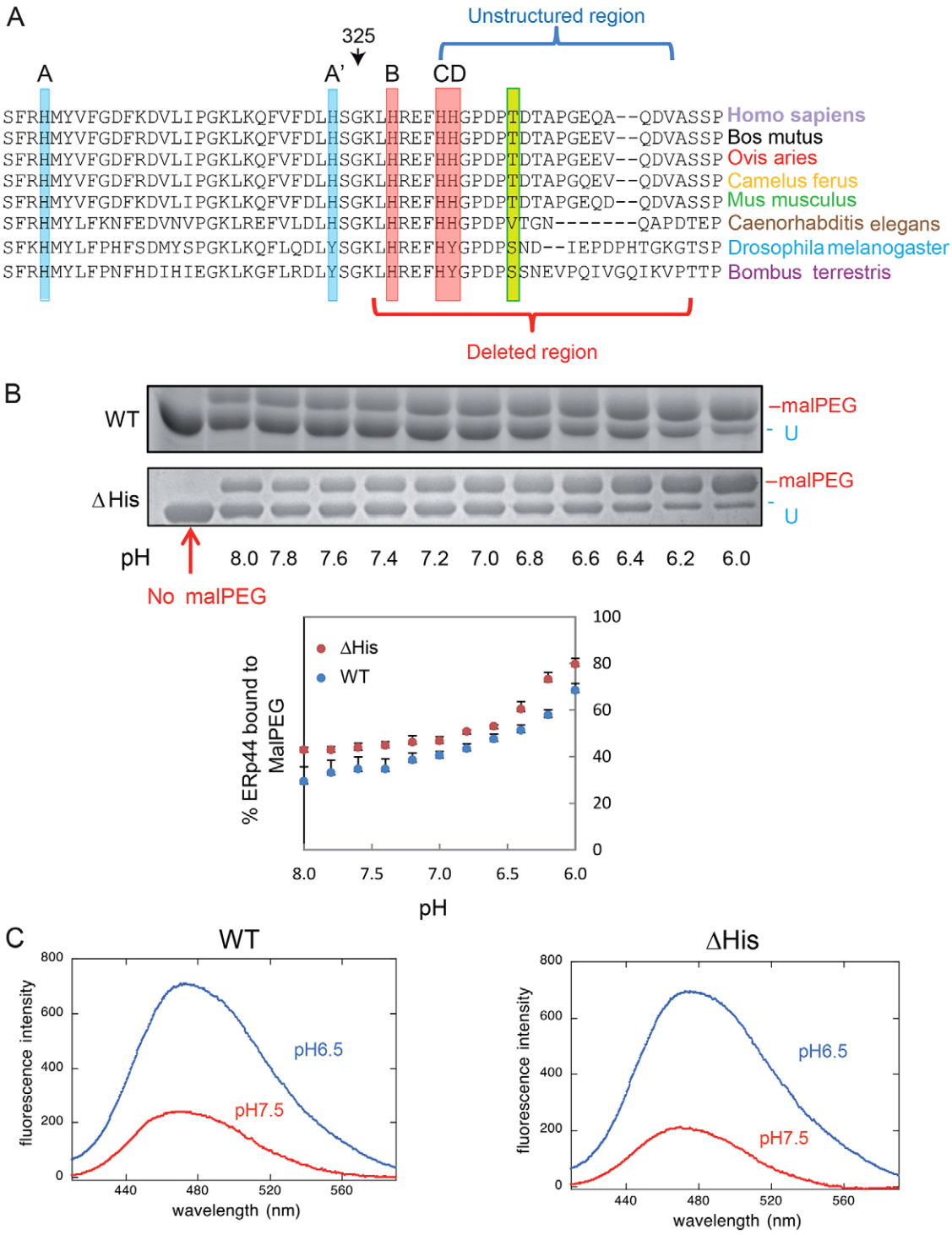

Fig. 1. pH-dependent conformational changes of ERp44 ΔHis *in vitro*. (A) Sequence conservation in the proximal part of the ERp44 C-tail. ClustalW2 alignment of the histidine-rich region and of the first part of the C-terminal tail of ERp44 reveals high sequence conservation in different organisms. Three histidine residues reside in the tail (B, C and D, highlighted here in red) and two in the domain-b′ (A and A′, in pale blue). A, B and C are the most conserved histidine residues, whereas A′ and D are absent in arthropods. The unstructured region in the crystal and the region deleted in the ΔHis mutant are indicated by blue and red brackets. (B) pH-dependent accessibility of ERp44 cysteine 29. Upon in vitro alkylation with MalPEG (10 min at room temperature), ERp44 undergoes an easily detectable mobility shift in SDS-PAGE, indicating the accessibility of C29 to MalPEG (upper two panels) (Vavassori et al., 2013). The percentage of MalPEG-bound ERp44 was plotted as a function of pH (lower panel). Clearly, lowering the pH increases the accessibility of C29 to MalPEG in the ΔHis mutant as well as in wt ERp44. (C) pH-dependent tail movements in wt and ΔHis ERp44 compared by ANS binding *in vitro*. ANS fluorescence spectra were measured for ERp44 wt or ΔHis. The exposure of hydrophobic surfaces correlates with increased and blue-shifted ANS fluorescence (Vavassori et al., 2013). In this assay, ERp44 wt and ΔHis also show similar pH-dependent changes.

Journal of Cell Science (2014) 127, 4260–4269 doi:10.1242/jcs.153239

efficiency (Vavassori et al., 2013). In the ΔHis mutant, the C-tail was still long enough to shield C29 and the surrounding hydrophobic patches at pH>7.0 (Fig. 1B,C). Even after deletion of the His-rich loop, however, more MalPEG was bound to ERp44 and the ANS fluorescence peak was blue-shifted and enhanced upon lowering the pH. These data suggested that *in vitro* C29 and the hydrophobic regions in ΔHis became exposed at pH values encountered in the Golgi (6.5), as we previously demonstrated for wild-type (wt) ERp44 (Vavassori et al., 2013).

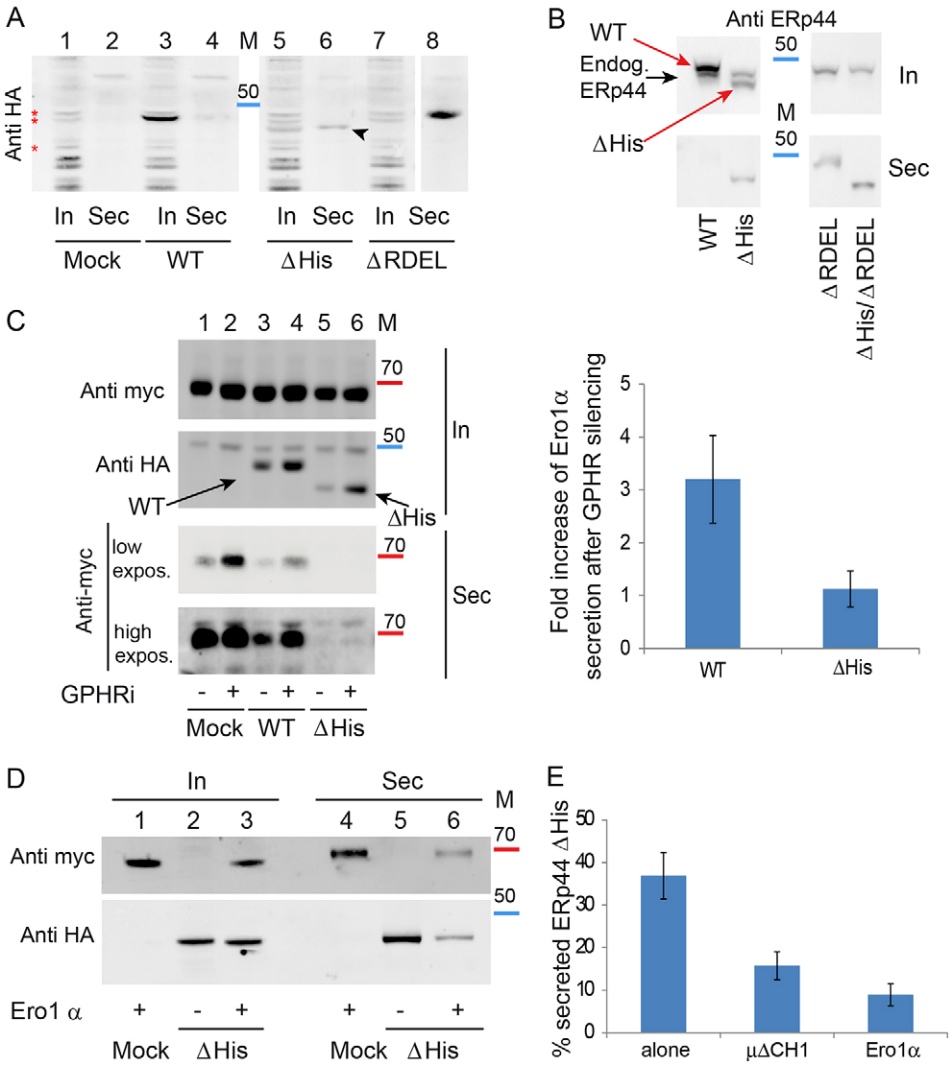

Fig. 2. The histidine-rich loop regulates accessibility of the active site and RDEL motif *in vivo*. (A) ERp44 mutants lacking the histidine-rich loop are secreted. The indicated HeLa transfectants were cultured for 4 h in fresh medium, and aliquots from lysates (In) and supernatants (Sec) analyzed under reducing conditions by western blotting with anti-HA antibodies. The first two lanes (Mock) show cells transfected with an empty plasmid. The arrowhead points at secreted ΔHis ERp44. Red asterisks point at background bands recognized by anti-HA antibodies. Albeit not elegant, these unwanted bands provide good loading controls. In all western blot analyses, molecular mass markers were used (see also Fig. 5): the red and blue bands indicate the migration of the 70- and 50-kDa markers. (B) Residual retention of ERp44 ΔHis is due to KDELR activity. Aliquots from lysates (In) and spent media (Sec) were collected from HeLa transfectants (treated as in A) and analyzed under reducing conditions by western blotting with monoclonal anti-ERp44 antibodies (36C9) that recognize also endogenous ERp44. The black and red arrows point to endogenous and HA-tagged overexpressed ERp44 molecules, respectively. Note that deletion of the C-terminal RDEL allows complete ΔHis secretion, whereas no endogenous ERp44 is detectable extracellularly. (C) ERp44 ΔHis is more efficient in retaining Ero1α in a pH-independent manner. HeLa cells were co-transfected with ERp44 variants and Ero1α as indicated and the pH gradient in the ESC was altered by GPHR silencing (– lanes show cells treated with irrelevant siRNA) as described previously (Vavassori et al., 2013). Aliquots from lysates (In) and culture media (Sec) were collected and analyzed by western blotting using sequential staining of the same filter with anti-HA and anti-Myc antibodies to detect ERp44 or Ero1α, respectively, as indicated. Note that less Ero1 is secreted out of cells expressing the ΔHis mutant, although its intracellular level is lower than that of wt ERp44. A higher exposure of the secreted samples is shown to detect the small amounts of Ero1α secreted out of cells expressing the ΔHis mutant. Intracellular and secreted proteins were quantified by densitometric analyses, and the mean fold of induction of Ero1α secretion upon GPHR silencing calculated relative to controls (right panel). Data represent the mean±s.d. of eight or more experiments like the one shown in the left panel. (D) Client-induced retention of ΔHis. Aliquots of lysates (In) and supernatants (Sec) of the indicated HeLa transfectants were analyzed as above. Note that much less ERp44 ΔHis is secreted in the presence of Ero1α, and vice versa. (E) Secretion of ERp44 ΔHis is inhibited by client proteins (Ero1α and μΔCH1). Secretion of ΔHis in the presence or absence of overexpressed Ero1α or μΔCH1 was analyzed as above. To quantify secretion, we calculated the ratios between the ΔHis bands detected extra- and intra-cellularly after 4 h cultivation in fresh medium. To facilitate the comparison amongst different transfectants, the values obtained for wt ERp44 and ΔRDEL were arbitrarily set at zero and 100, respectively. Histograms show the mean±s.d. for three or more experiments.

Journal of Cell Science (2014) 127, 4260–4269 doi:10.1242/jcs.153239

The histidine-rich loop regulates the accessibility of the active site and RDEL motif *in vivo*

Even though ERp44 ΔHis behaved similarly to wt ERp44 *in vitro*, the mutant did show evident phenotypes *in vivo*. Indeed, ΔHis was partially secreted by HeLa cells (Fig. 2A, lane 6, black arrowhead), suggesting lower RDEL accessibility. Accordingly, the double mutant ΔHis/ΔRDEL was secreted at levels similar to ERp44 ΔRDEL (Fig. 2B). Pulse-chase assays (supplementary material Fig. S2A) confirmed that the ΔHis mutant was secreted by HeLa transfectants, and not degraded to a significant extent. Taken together, these findings indicate that in the absence of the histidine loop the RDEL motif interacts less efficiently with its cognate receptors.

Next, we investigated whether the ΔHis mutant maintained the ability to prevent the secretion of Ero1α. Like Prx4, Ero1α also lacks a KDEL motif and is retained inside cells through interactions with PDI or ERp44 (Kakihana et al., 2013; Otsu et al., 2006). Secretion assays clearly demonstrated that: (i) ΔHis was in part secreted (Fig. 2A), (ii) ΔHis was more efficient than

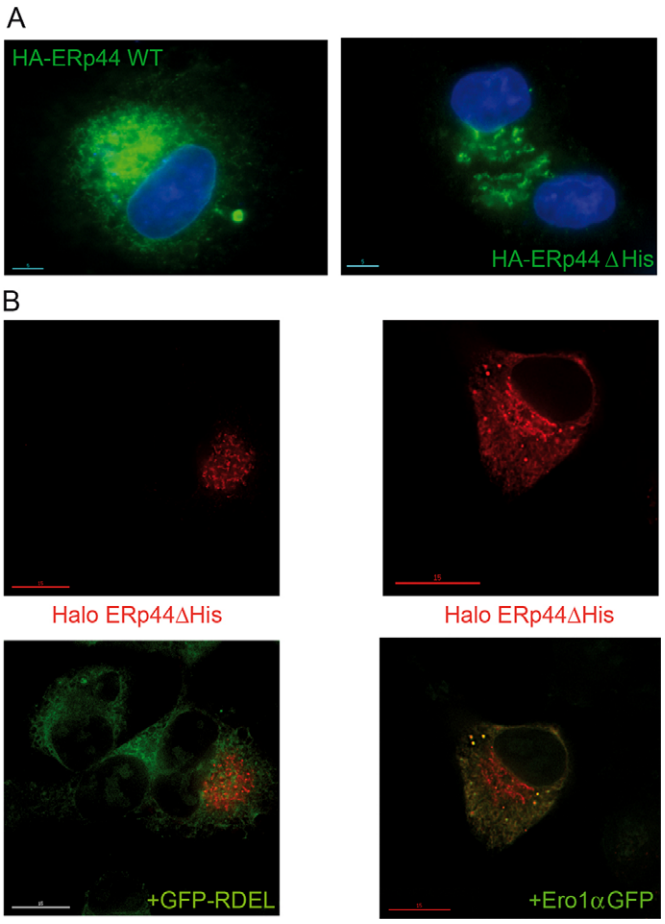

Fig. 3. Deletion of histidine-rich loop favors accumulation of ERp44 in distal ESC stations. (A) Steady-state localization. HepG2 transfectants expressing HA-tagged wt and ΔHis ERp44 were analyzed by immunofluorescence with anti-HA antibody (green). The blue staining (DAPI) was used to detect nuclei. Note that much less green staining is detected in the nuclear membrane or peripheral ER in ΔHis transfectants, as compared to cells expressing wt ERp44. (B) Client-induced relocalisation of ΔHis to the ER. Co-expressing Ero1α–GFP, but not sGFP–RDEL, causes the re-localization of ΔHis in the ER. HepG2 cells were co-transfected with Halo-tagged ERp44 ΔHis and sGFP–RDEL or Ero1α–GFP and then decorated with a Halo ligand (red signal). Clearly, no colocalization is detectable between sGFP–RDEL (green) and ERp44 ΔHis (red), whereas expression of Ero1α–GFP also causes ΔHis to localize in the ER, yielding a reticular yellow staining (bottom right panel). Scale bars: 5 μm (A); 15 μm (B).

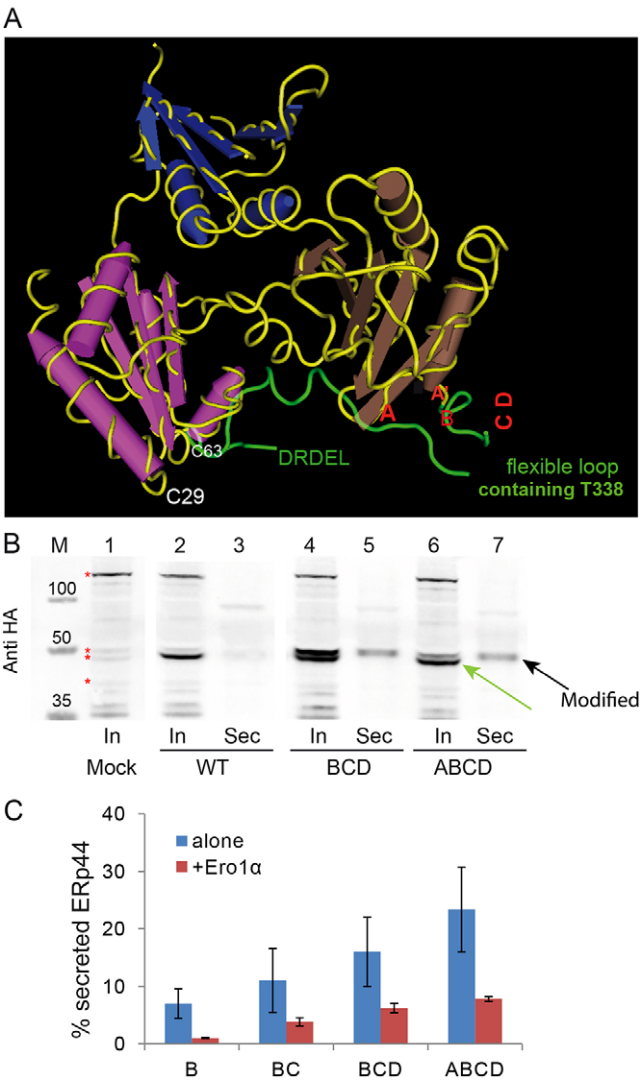

Fig. 4. Replacing conserved histidines causes O-glycosylation and secretion of ERp44. (A) 3D localization of conserved histidine residues. The panel highlights the 3D crystal structure of ERp44 with the C-tail in green. Red letters (A, A′, B, C and D) point at the position of the five histidine residues. Histidine residues C and D are located at the beginning of an unstructured histidine loop (332–350) which, as the five C-terminal DRDEL residues, is not resolved in the crystal. (B) Replacement of histidine residues induces secretion of modified ERp44. Aliquots from lysates (In) and culture media (Sec) were collected from HeLa transfectants expressing the indicated ERp44 variants and blots were stained with anti-HA antibody. Similar experiments were performed for other histidine mutants (data not shown). Note that anti-HA antibodies specifically detect two bands in the lysates of the BCD and ABCD mutants, of which only the upper one is secreted (black arrow). The green arrow points at the only intracellular band recognized in transfectants expressing wt ERp44. Red asterisks point at some background bands recognized by anti-HA antibodies, which provide useful loading controls. (C) His replacement mutants are retrieved more efficiently upon Ero1α co-expression. ERp44 secretion was quantified as described in Fig. 2E in HeLa cells expressing the indicated ERp44 mutants alone or with Ero1α. The histograms show the percentage of secreted ERp44 for the different mutants. The data represent the mean±s.d. of three or more experiments in the presence of Ero1α. Secretion efficiency was calculated as described in legend to Fig. 2E.

Journal of Cell Science (2014) 127, 4260–4269 doi:10.1242/jcs.153239

wt ERp44 in preventing Ero1α secretion (Fig. 2C, lanes 3 and 5), and (iii) paradoxically, the co-expression of a client (Ero1α) inhibited the secretion of the retainer (ΔHis, Fig. 2D, lanes 5 and 6). These findings suggest that client binding could favor RDEL exposure in ΔHis. The 'client-induced retention' of ΔHis was evident upon co-expressing not only Ero1α (Fig. 2E) but also Ig-μΔCH1, another known ERp44 substrate (Anelli et al., 2007; Ronzoni et al., 2010; Vavassori et al., 2013).

To analyze the pH dependency of ΔHis in living cells, we silenced the Golgi pH regulator [GPHR (Maeda et al., 2008)], specifically raising the pH in the Golgi (Vavassori et al., 2013). Owing to the unavailability of anti-GPHR antibodies, the efficiency of silencing was monitored by RT-PCR assays (supplementary material Fig. S2B). As previously observed (Vavassori et al., 2013), neutralizing the ER–Golgi pH gradient allowed Ero1α secretion (Fig. 2C, lanes 1 and 2), as was the case in cells overexpressing wt ERp44 (Fig. 2C, lanes 3 and 4). In contrast, basification of the cis-Golgi did not affect the capability of ΔHis to retain Ero1α (Fig. 2C, lanes 5 and 6).

Thus, deletion of histidine-rich loop allowed secretion of ERp44 unless high-affinity client proteins were co-expressed. At the same time, it increased its ability to retain Ero1α (Fig. 2C) and Ig-μΔCH1 (data not shown) and limited its pH dependency (Fig. 2C). Secreted Ero1α could be detected only upon overexposure of the Western blot, such was the efficiency of ΔHis in retaining the oxidase.

Deletion of histidine-rich loop favours accumulation of ERp44 in distal ESC stations

How could ERp44 ΔHis be so efficient in retaining Ero1α? Endogenous ERp44 is mainly localized in the ERGIC and cis-Golgi, partly owing to interactions with the lectin ERGIC-53 (Anelli et al., 2007). In contrast, overexpressed ERp44 accumulates in the ER (Anelli et al., 2002; Anelli et al., 2003). The ΔHis mutant localized more distally than wt ERp44 when expressed in the secretory HepG2 cell line (Fig. 3A). Organelle fractionation assays confirmed that ΔHis accumulated in the ERGIC and cis-Golgi, a localization that would favor capture of clients destined to be retrieved (data not shown).

Based on the earlier observation that overexpression of high-affinity client proteins prevented secretion of ΔHis, we investigated whether the presence of Ero1α–GFP could alter the subcellular localization of the ΔHis mutant. An ER-resident protein that does not bind ERp44 (sGFP–RDEL) was used as a control (Fig. 3B). Clearly, the co-expression of Ero1α–GFP, but not sGFP–RDEL, caused re-localization of ΔHis into the ER. These data reinforced the notion that interactions with high-affinity clients (e.g. Ero1α) keep the tail of ERp44 in an open conformation, favoring RDEL exposure and KDELR-dependent retrieval of the complex to the ER.

Conserved histidines regulate C-tail movements *in vivo*

Considering their conservation from *Homo sapiens* to *Caenorhabditis elegans* (Fig. 1A), we replaced histidine residues 299, 323, 328, 332 and 333 (called hereafter A, A′, B, C or D, respectively) with alanine residues, singularly or in combinations. The A and A′ residues are part of the domain-b′, whereas residues B, C and D are located in the C-tail (Wang et al., 2008). Histidine residues A, A′ and B are part of structured 3_{10} helices whereas histidine residues C and D reside in a flexible loop (Fig. 4A) and are hence most likely to be exposed to the solvent. A, B and C are conserved throughout evolution. Single mutation of each of them allowed partial secretion. In contrast, replacing the less conserved histidine residues, A′ or D, had little, if any, effect (Table 1; data not shown). Clearly, the more histidine residues were replaced, the more ERp44 was secreted (Fig. 4B,C). Deleting the entire loop had even stronger effects (Fig. 2A). Taken together, these results suggest that in living cells the flexible His-rich loop is important to favor tail movements leading to RDEL exposure in the absence of high-affinity clients. Without this loop, the RDEL motif likely remains less accessible to cognate receptors and as a consequence the mutant is secreted. By contrast, co-expression of Ero1α

Table 1. Phenotypic characterization of ERp44 histidine mutants

	Ero1α retention[a]		ERp44 secretion[b]			
ERp44 variant	Untreated	GPHRi	Alone	Ero1α	O-glyc.	Subcellular localization[c]
WT	++	+	Undetectable	Undetectable	No	ER–ERGIC
ΔRDEL	−	−	100%[c]	100%	Yes	Barely detectable
ΔHis	++++	++++	36%	9%	No	ERGIC–cis-Golgi
A	++	ND	<10%	Undetectable	Yes	ND
A′		ND	<5%	Undetectable	Yes	ND
B	++	ND	<10%	No	Yes	ER–ERGIC
C	ND	ND	<10%	ND	Yes	ER–ERGIC
D	+	ND	<5%	Undetectable	Yes	ER–ERGIC
BC	++	ND	≈10%	<5%	Yes	ERGIC
BD	+	ND	<10%	Undetectable	Yes	ND
CD	+++	++	<10%	Undetectable	Yes	ERGIC
BCD	+++	ND	15–20%	≈5%	Yes	ERGIC–cis-Golgi
A′BCD	+++	ND	≈10%	≈5%	Yes	ND
ABCD	+++	ND	20–25%	<10%	Yes	ERGIC–cis-Golgi

The data summarize the main features of the mutants described in this paper, including the capability of retaining overexpressed Ero1α, and of being secreted in different conditions, and their basal subcellular localization. GPHRi , GPHR-silenced cells; ND, not determined.

[a]Scoring is relative to the mutants with the highest (ΔHis ++++) and lowest (ΔRDEL −) efficiency. The former efficiently retains Ero1 even when expressed at rather low levels (see Fig. 2C).

[b]For ERp44 secretion, scoring is relative to a maximum (100%, ΔRDEL) and a minimum (0%, wt ERp44), which is undetectable in the spent media (4 h) of our HeLa transfectants. Precise values are given only for ΔHis, for which the experiment has been repeated over 10 times.

[c]Subcellular localization was determined by immunofluorescence, based on data like those shown in Fig. 3 and and supplementary material Fig. S3. Owing to its rapid secretion (Anelli et al., 2007), the DRDEL mutant is not easily detectable inside cells unless radioactive pulse-chase assays are utilized (see supplementary material Fig. S2).

Journal of Cell Science (2014) 127, 4260–4269 doi:10.1242/jcs.153239

strongly inhibited secretion of the mutants (Fig. 4C), as described earlier for ΔHis (Fig. 2D). Given that ERp44 is a pH-regulated chaperone, it is not surprising that the histidine residues (whose intrinsic pK_a is near neutral) contained in or immediately upstream the loop contribute to the control of RDEL exposure *in vivo*. In line with their high evolutionary conservation, histidine residues A, B and C appear to be particularly important in regulating tail movements.

Secreted ERp44 is O-glycosylated at threonine 338

Western blotting analyses revealed the presence of two bands in the lysates of the BCD and ABCD mutants, of which only the upper was secreted (Fig. 4B, see arrows). Although ERp44 has no potential N-glycosylation sites, mutants that escaped KDELR-dependent retrieval could undergo O-glycosylation in the Golgi. To ascertain whether this was indeed the case, we treated HeLa transfectants with brefeldin A (BFA), a drug known to induce the retrograde transport of Golgi enzymes to the ER (Lippincott-Schwartz et al., 1989). The electrophoretic mobility of wt and BCD ERp44, but not of ΔHis, was lower after BFA treatment (Fig. 5A, compare lanes 3, 7 and 10). Treatment with O-glycosidase restored faster migration (lane 4) and abolished the doublet observed in the BCD mutant (lane 9), demonstrating that ERp44 can undergo O-glycosylation before being secreted. In contrast, ΔHis ERp44 was not modified in the presence of BFA, indicating that either the target residue was deleted in this mutant or the replacement caused its inaccessibility to O-glycosyl transferases.

Notably, endogenous ERp44 was also modified upon BFA treatment (Fig. 5B, see black arrow). Non-reducing gels revealed that O-linked glycosylation did not prevent ERp44 from forming covalent complexes with its clients (Fig. 5B, see lanes 3 and 4). The fact that most wt ERp44 was not modified in normal conditions implied its retrieval before the modification occurs. *In silico* prediction programs (Hamby and Hirst, 2008; Steentoft et al., 2013) pointed at threonine residues 338 and 340 as possible substrates of O-glycosylation. Both are located within the loop deleted in ΔHis, which would explain why this mutant is not O-glycosylated. Replacing the most conserved one, T338, with alanine in a mutant that was in part secreted and modified (ABCD) was sufficient to prevent the processing (Fig. 5C, lanes 5 and 6). Failure to undergo O-glycosylation did not prevent secretion (Fig. 5D). Thus, ERp44 can be O-glycosylated at T338.

Despite the fact that in the experiment shown in Fig. 4B the BCD and ABCD mutants were secreted at similar levels, more O-glycosylated accumulated intracellularly in the former mutant.

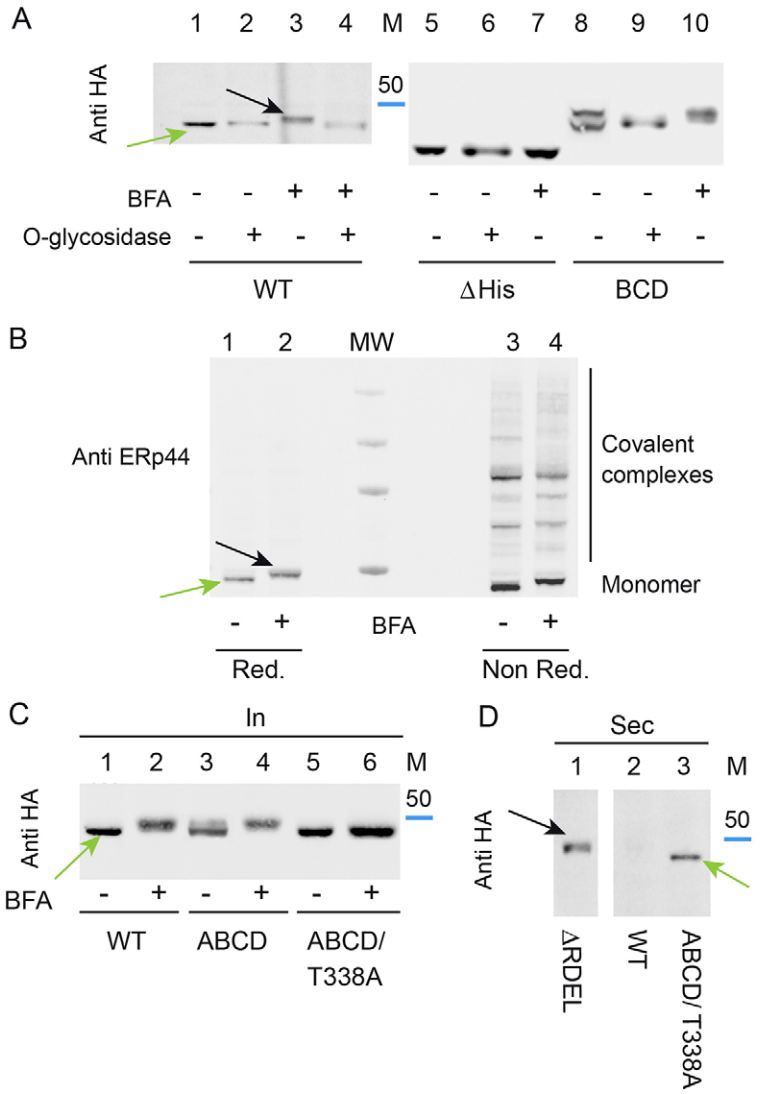

Fig. 5. Mapping client-induced retrieval of His replacement mutants with respect to O-glycosylation. (A) Secreted ERp44 is O-glycosylated. HeLa cells transfected as indicated were treated with (lanes 3, 4, 7, 10) or without brefeldin A (BFA) for 4 h to determine whether retrieval of Golgi enzymes to the ER caused processing of ERp44. Aliquots from the lysates were digested with (lanes 2, 4, 6, 9) or without O-glycosidase (see Materials and Methods), resolved by gel electrophoresis and blots stained with anti-HA antibody. The blue band indicates the migration of the 50-kDa marker. (B) Endogenous ERp44 can also be O-glycosylated and form covalent complexes with client proteins. Untransfected HeLa cells were treated with BFA as above and resolved under reducing (lanes 1–2) and non-reducing (lanes 3–4) conditions before blotting and staining with 36C9 monoclonal anti-ERp44 antibodies. Molecular mass markers (250, 130, 70 and 50 kDa) are shown in the center lane (MW). (C) ERp44 is O-glycosylated on threonine 338. Aliquots from the lysates of the indicated HeLa transfectants treated with or without BFA were analyzed by western blotting with anti-HA antibody. (D) Replacing threonine 338 does not impede secretion of the ABCD mutant. The supernatants of cells transfectants were resolved under reducing conditions and stained with anti-HA antibody. The green arrow points at the secreted product of the T338A. This mutant displays faster mobility than the O-glycosylated ΔRDEL secretory products (black arrow).

Journal of Cell Science (2014) 127, 4260–4269 doi:10.1242/jcs.153239

These findings suggest that BCD could also be more efficiently retrieved from stations downstream the compartment where O-glycosylation takes place. The lower pH of these downstream stations could increase the exposure of RDEL (Vavassori et al., 2013) and/or the activity of KDELR (Wilson et al., 1993).

Exploiting O-glycosylation to map where ERp44 binds its clients

As described in Fig. 2D and Fig. 4C, overexpression of high-affinity ERp44 clients prevented the secretion of histidine mutants, likely increasing RDEL accessibility. The notion that these histidine mutants could be O-glycosylated prompted us to determine whether the binding of different clients occurred before or after the compartment where this modification takes place. Substrates binding before encountering the glycosylating enzymes would increase the lower molecular mass band accumulating in cell lysates, whereas O-glycosylated forms would prevail if the interaction occurred in downstream stations. The ABCD mutant was hence expressed with Ero1α, Prx4, Ig-μΔCH1, adiponectin or Sumf1, and the unmodified:modified band ratios were calculated (Fig. 6A). Clearly, expression of Ero1α and Prx4 favored accumulation of the unglycosylated species. In contrast, Sumf1 induced retrieval of ABCD after it had been processed by O-glycosyl transferases. μΔCH1 and adiponectin had intermediate effects (Fig. 6B). These observations might reflect differences in the binding affinities or pH dependency of the interactions between

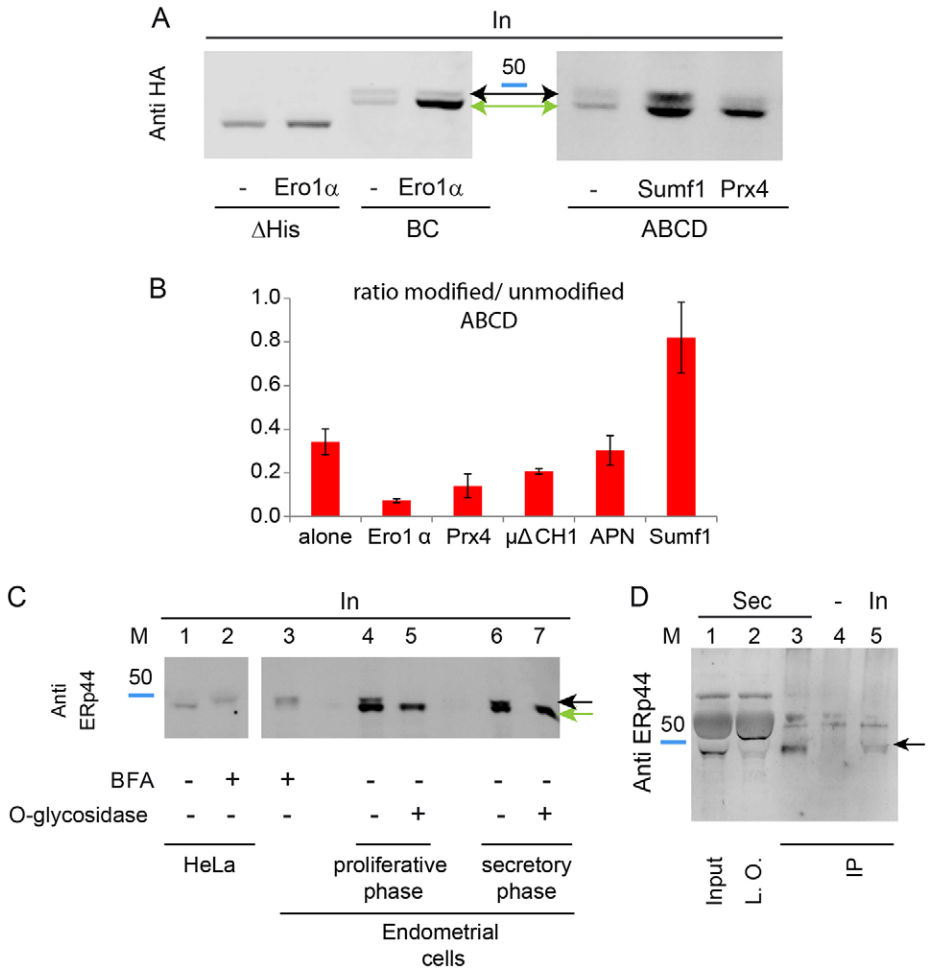

Fig. 6. Client-induced retrieval of ERp44. (A) Sumf1 can also bind ERp44 after O-glycosylation. HeLa cells were co-transfected as indicated. Aliquots from the lysates were then resolved by SDS-PAGE and blots stained with anti-HA. Note the accumulation of non-glycosylated histidine mutants in the lysates of cells co-expressing Ero1α or Prx4. Instead, Sumf1 expression allows significant accumulation of O-glycosylated ABCD ERp44. (B) Sequential client-induced retrieval of ERp44 histidine mutants. The histograms show the ratio between modified and unmodified ABCD ERp44 in the presence of Ero1α, Prx4, Sumf1, Ig-μΔCH1 or adiponectin (APN). Data represent the mean±s.d. of three or more experiments. (C) Endogenous ERp44 is O-glycosylated in primary endometrial cells. Aliquots of the lysates obtained from endometrial cells in their proliferative (lanes 4–5) or secretory (lanes 3, 6–7) phase (Di Blasio et al., 1995) were digested with (lanes 5, 7) or without (lanes 3, 4, 6) O-glycosidase and resolved by gel electrophoresis under reducing conditions. Note that upon digestion, the doublet visible in untreated samples collapses into a single higher mobility band, which comprises un-glycosylated and de-glycosylated ERp44 (green arrow). The black arrow points at the O-glycosylated species, the main form accumulating in HeLa (lane 2) or endometrial (lane 3) cells after treatment with BFA. (D) Endogenous ERp44 is secreted by endometrial stromal cells. Aliquots from the lysates or spent media (48 h) corresponding to 8×10^4 or 7×10^5 endometrial cells in their secretory phase were immunoprecipitated (IP) with the 36C9 monoclonal anti-ERp44 antibody, resolved under reducing conditions and stained with rabbit anti-ERp44 antibody (JDA1). Lanes 1 and 2 show one-third of the spent medium before (Input) or after (L.O., left over) immunoprecipitation. The band migrating above the 50-kDa marker is BSA, which is highly abundant in fetal calf serum. Cross-linked beads were used as a negative control (lane 4). Endogenous ERp44 is clearly detectable in the culture medium and migrates with a molecular mass similar to the O-glycosylated ERp44 species present intracellularly (black arrow).

Journal of Cell Science (2014) 127, 4260–4269 doi:10.1242/jcs.153239

ERp44 and its clients. In addition, other factors, including molecules binding to the histidine-rich region, could regulate the strength and location of the interactions between ERp44 and its clients.

The above data demonstrated that certain ERp44 mutants could be O-glycosylated. To verify the physiological relevance of ERp44 processing, we screened a wide panel of cell lines and tissues (E. Yoboue, T.A., S.S. and R.S., data not shown). ERp44 yielded a doublet band in primary endometrial cells obtained from normal volunteers (Fig. 6C, lanes 4 and 6). The mobility of the upper band (highlighted by a black arrow) is comparable to the one accumulating upon treatment with BFA (lanes 2 and 3). Treatment with O-glycosidase collapsed the doublet into a single band (lanes 5–7, see green arrow), confirming that endogenous ERp44 can undergo O-glycosylation. Notably, the relative abundance of O-glycosylated ERp44 was higher in endometrial cells in the secretory phase than in the proliferative phase (Di Blasio et al., 1995). Processed ERp44 was detected in the spent medium of secretory endometrial cells (Fig. 6D, lanes 1 and 3).

DISCUSSION

To promote productive folding, chaperones must bind and release their clients. Some are regulated by ATP and others by the redox state, whereas ERp44 exploits the pH gradient existing between the ER and the Golgi (Vavassori et al., 2013, and references therein). How does ERp44 sense pH? We show here that highly conserved histidine residues in the ERp44 C-tail provide a second sensing device that acts coordinately with the C29 protonation mechanism previously shown to regulate ERp44 cycling and activity within the ESC (Vavassori et al., 2013).

Deletion or replacement of the key conserved ERp44 histidine residues had notable consequences *in vivo*. In fact, it caused secretion of the histidine mutants by the cells, likely owing to a reduced accessibility of the RDEL motif to KDELR in the Golgi. Accordingly, co-expression of clients that would bind to the SBS and force RDEL exposure restored their retrieval (see Fig. 7). In contrast, deletion or mutation of the conserved histidine residues had marginal effects *in vitro* (Fig. 1A, and our unpublished results), indicating that additional 'histidine-region-binding factors' regulate ERp44 *in vivo* (Fig. 7). Such factors could bind ERp44 in the ER and limit its forward transport, accounting for the enrichment of the histidine mutants in post-ER compartments (Fig. 3). Alternatively, the mutants might be present and/or be activated in distal compartments to assist in tail opening (and consequent RDEL exposure) in the absence of clients. Thus, whereas the C29-based tail regulation is intrinsic to ERp44 and can be revealed *in vitro*, the histidine-dependent mechanisms are evident only *in vivo* as they require additional regulatory elements.

Histidine mutants are more efficient than wt ERp44 in preventing Ero1α secretion. This feature was rather unexpected because they are partly secreted, and might reflect their increased specificity towards Ero1α. Some clients would be more effective than others in competing with the C-tail for the substrate-binding site in the histidine mutants, which likely have a higher kinetic barrier for tail opening. In this context, Ero1 and Prx4 bind to ERp44 mainly before it undergoes O-glycosylation, whereas Sumf1 can also interact afterwards (Fig. 6A,B). These observations suggest that different proteins could be deposited sequentially in the exocytic pathway, depending on their affinity for ERp44 or on the pH dependency of the chaperone–client interaction. Along these lines, it is interesting that most ERp44

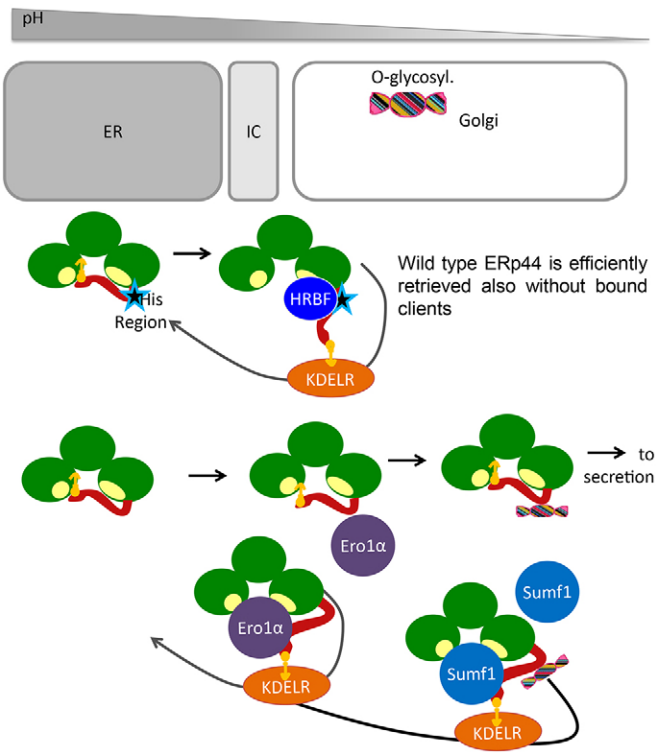

Fig. 7. Schematic model of ERp44 regulation. The lower pH encountered by ERp44 as it proceeds along the early secretory pathway, favors opening of the C-tail and KDELR binding regardless of the presence or absence of high-affinity client proteins. Accordingly, ERp44 mutants that bind few, if any, substrates in cells (e.g. ERp44C29S; Anelli et al., 2003) are not secreted. By contrast, mutants lacking key conserved histidine residues or a loop at the border between the domain-b′ and the tail (star) bind poorly to KDELRs, proceed towards the extracellular space and are O-glycosylated. Client binding induces KDELR-dependent retrieval of histidine mutants before (Ero1, Prx4) or after (Sumf1) O-glycosylation takes place. Given that histidine mutants remain pH sensitive *in vitro*, we hypothesize that histidine-region binding factor(s) (HRBF) favor tail movements *in vivo*, allowing efficient RDEL exposure.

substrates and/or partners that are ER-resident enzymes (Ero1α, Prx4 and Sumf1) lack a C-terminal KDEL sequence and rely on protein–protein interactions for their intracellular localization. Thus, the relative abundance of ERp44 is likely to regulate their localization and activity in and between different cells (Pagani et al., 2001; Swiatkowska et al., 2010; Zito et al., 2007).

Consistent with its many intracellular functions (Cortini and Sitia, 2010), ERp44 is efficiently retained by most of the cell types analyzed. Notably, however, endometrial cells secrete O-glycosylated ERp44 and do so more efficiently in the secretory phase of the menstrual cycle (Fig. 6C,D). These findings also suggest possible role(s) for ERp44 in intercellular dialogues. Accordingly, ERp44 can be released by platelets following activation (Holbrook et al., 2010). It is thus possible that other mechanisms, including pH regulation, regulate the localization of ERp44 and in turn of many of its clients and interactors. Controlling the release of ERp44 might have relevant pathophysiological implications.

MATERIAL AND METHODS

Reagents and cell cultures

Chemicals were from Sigma, unless otherwise indicated. Monoclonal and polyclonal anti-ERp44 antibodies (36C9 and JDA1 respectively),

anti-Myc (9E10) and anti-GM130 were as previously described (Anelli et al., 2002; Anelli et al., 2007). Polyclonal anti-PDI was a kind gift of Ineke Braakman (Utrecht, The Netherlands). Unconjugated goat anti-mouse-Ig antibodies were from Southern Biotechnology Associates, Inc. (Birmingham, AL), and horseradish peroxidase (HRP)-bound goat anti-mouse-Ig and anti-rabbit-Ig were from Jackson ImmunoResearch Laboratories, Inc. Fluorescent goat anti-mouse- and anti-rabbit-IgG (H^+L) conjugated to Alexa Fluor 700, 647, 546 and 488 were from Invitrogen Molecular Probes (Eugene, Oregon, USA).

HeLa and HepG2 cell lines were purchased from the ATCC. Tissue culture, transfection, and silencing were performed as described previously (Anelli et al., 2007). HepG2 cells were transfected by FugeneHD (Promega Corporation, Madison, USA) following the manufacturer's instructions. Primary endometrial cells were collected from healthy donors and cultured as described by Di Blasio at al. (Di Blasio at al., 1995). All women provided informed consent for their clinical data and samples to be used for research purposes. The San Raffaele Hospital Ethical Committee approved the study protocol.

Plasmids and vectors

The cDNA encoding human ERp44 without the signal sequence from pGEX-4T-1-ERp44 and the vector for sGFP–RDEL expression were as previous described (Vavassori et al., 2013). Vectors driving the expression of human ERp44 were as previously described (Anelli et al., 2002). Mutants were obtained by PCR or by site-directed mutagenesis (SDM) using the primers listed in supplementary material Table S1. All the primers were purchased from PRIMM srl (Milano, Italy). Plasmids encoding mutated secretory Ig-μ chains (μΔCH1) were as previously described (Cenci et al., 2006; Mattioli et al., 2006).

Halo ERp44 vector construction

A Halo tag was inserted after the ERp44 leader sequence cleavage site as follows: ERp44 without tags was cleaved from the pcDNA3.1 (−) vector by XhoI and KpnI and inserted in pBlueScript II KS (+). A SgfI site was inserted after the leader sequence cleavage site by PCR (p44sgfI Fw, 5′-CCTGTAACAACTGAAATAGCGATCGCTGAAATAACAAGT-3′ and p44sgfI Rv, 5′-ACTTGTTATTTCAGCGATCGCTATTTCAGTTGTT-ACAGG-3′). The PCR product was then re-inserted into pcDNA 3.1 (−) vector following XhoI and KpnI digestion. In pHTN-HaloTagCMV-neoVector® (Promega Corporation), HaloTag was mutagenized inserting a SgfI site at the N-terminal extremity by PCR (pHTN SgfI Fw, 5′-GCCGCGATCGCTGAAGCAGAAATCGGTAACTGGCTTTCCATTC-3′ and pHTN SgfI Rv: 5′-GGAAGCGATCGCGTTATCGCTCTG-3′). Halo-ERp44 was obtained by ligating SgfI fragments overnight at 16℃, which were then screened by SmaI digestion and validated by sequencing.

Western blotting, densitometric quantifications and biochemical techniques

Fluorograms or western blot images were acquired with the Chemidoc-it Imaging System (UVP, Upland, CA) or with FLA-900 Starion (Fujifilm Life Science, USA) and quantified with Image J as described previously (Anelli et al., 2007).

To assess O-glycosylation, aliquots from HeLa cell lysates were denatured at 95℃ for 10 min in glycoprotein denaturing buffer (New England BioLabs Inc.), digested with neuraminidase and O-glycosidase overnight at 37℃ and analyzed by western blotting with specific antibodies.

As loading controls for western blotting assays, we used Ponceau and/or anti-tubulin antibody staining. In some experiments, some nonspecific bands were present in blots stained with anti-HA antibody (see for instance red asterisks in Figs 2 and 4). Signal intensity was quantified with Image J. The loading of the lanes rarely, if ever, differed more than 5%, with the exception for O-glycosidase treatment where the protein levels were about 20% lower with respect to BFA or untreated samples.

Immunoprecipitation of endogenous ERp44 from primary endometrial cell lysates and spent medium was performed with Sepharose-immobilized 36C9 as previously described (Anelli et al., 2012).

Wild-type and mutant ERp44 were purified and analyzed as described previously (Masui et al., 2011; Vavassori et al., 2013). Briefly, ANS fluorescence spectra were recorded in 1-cm cuvettes on a Hitachi F-2500 spectrofluorometer. ERp44 and mutants (5 μM) were mixed with 100 μM ANS in 20 mM Tris-HCl (pH 7.5) or MES (pH 6.5) containing 150 mM NaCl and incubated at 20℃ for 10 min before measurement.

For maleimidyl PEG-2K modification of ERp44 C29, each ERp44 derivative (5 μM) was incubated on ice for 30 min in various pH buffers containing 100 mM sodium phosphate and 150 mM NaCl, followed by incubation with maleimidyl PEG2K (300 μM) for 10 min at room temperature. The reaction was stopped by the addition of 5% trichloroacetic acid, and the protein pellet was washed with acetone and dissolved in buffer containing 50 mM Tris-HCl (pH 7.0) and 1% SDS before loading onto a reducing SDS gel (10%).

Radioactive pulse-chase assays

Cells were starved for 5 min in cysteine- and methionine-free DMEM (GIBCO, Invitrogen), pulsed for 10 min with [^{35}S]cysteine and [^{35}S]methionine (Easy Tag, Perkin-Elmer), washed twice and chased in complete medium. After the indicated chase times, cells were treated with 10 mM NEM and lysed in RIPA buffer as described previously (Vavassori et al., 2013). Immunoprecipitates were resolved by SDS-PAGE under reducing conditions, transferred onto nitrocellulose and filters visualized by autoradiography with FLA900 Starion (Fujifilm Life Science, Tokyo, Japan).

Immunofluorescence

HepG2 cells were plated on 15-mm glass coverslips and transfected. After 48 h of transfection, cells were fixed in 4% PFA, permeabilized with 0.2% Triton X-100 and stained with different antibodies. For Halo-tagged proteins, cells were incubated overnight with 10 nM TMR Halo ligand (Promega Corporation). Samples were analyzed on an Olympus inverted fluorescence microscope (model IX70) with DeltaVision RT Deconvolution System (Alembic, HSR, Milano). After deconvolution, images were processed with Adobe Photoshop CS4 (Adobe Systems Inc.).

GPHR silencing

Total RNA from untreated and GPHR silenced (GPHRi) HeLa transfectants was extracted with Tryzol from Thermo Fisher Scientific (Waltham, USA) following the manufacturer instructions and its quality was checked by OD_{260}:OD_{280} readings and electrophoresis. An aliquot of each sample was retro-transcribed by Super-Script II kit (Invitrogen, USA). Real-time PCR was performed with Syber green Master Mix in 25 μl of volume by ABI7900 (Applied Biosystem, Foster City, CA). Finally data were analyzed by SDS 2.1 software (Applied Biosystem).

Acknowledgements

We thank Stefano Vavassori (Université de Lausanne, CH-1066 Epalinges, Switzerland) for his contribution in designing and producing the ΔHis mutant, and for many stimulating discussions. We are indebted to Maria Francesca Mossuto, Anna Rubartelli, Eelco van Anken, Edgar Yoboue and other members of our laboratories for suggestions, criticisms and reagents, the Alembic facility for help in imaging and Roberta Colzani for secretarial assistance. We specially thank Paola Panina and Federica Quattrone (Division of Genetics and Cell Biology, IRCCS Ospedale San Raffaele) for kindly providing primary endometrial cells and for most helpful discussions.

Competing interests

The authors declare no competing interests.

Author contributions

S.S. performed most of the *in vivo* experiments, with the continuous help of T.A. M.C. analyzed the efficiency of substrate retrieval by the different mutants. S.M. and K.I. performed the *in vitro* experiments. C.F. was responsible for the pulse-chase assays and reagent optimization. With the fundamental help of K.I., T.A., M.D. and S.S., R.S. designed the strategy and coordinated the work described herein.

Funding

This work was supported by grants from Telethon [grant number GGP11077]; Associazione Italiana Ricerca sul Cancro (AIRC) [grant number IG 10721 and 5×1000 Special Project 9965 to R.S.]; the Japan Society for the Promotion of Science (JSPS) to S.M.; and the Next Generation World-Leading Researchers program (MEXT) to K.I.

Supplementary material

Supplementary material available online at
http://jcs.biologists.org/lookup/suppl/doi:10.1242/jcs.153239/-/DC1

References

Anelli, T., Alessio, M., Mezghrani, A., Simmen, T., Talamo, F., Bachi, A. and Sitia, R. (2002). ERp44, a novel endoplasmic reticulum folding assistant of the thioredoxin family. *EMBO J.* **21**, 835-844.

Anelli, T., Alessio, M., Bachi, A., Bergamelli, L., Bertoli, G., Camerini, S., Mezghrani, A., Ruffato, E., Simmen, T. and Sitia, R. (2003). Thiol-mediated protein retention in the endoplasmic reticulum: the role of ERp44. *EMBO J.* **22**, 5015-5022.

Anelli, T., Ceppi, S., Bergamelli, L., Cortini, M., Masciarelli, S., Valetti, C. and Sitia, R. (2007). Sequential steps and checkpoints in the early exocytic compartment during secretory IgM biogenesis. *EMBO J.* **26**, 4177-4188.

Anelli, T., Bergamelli, L., Margittai, E., Rimessi, A., Fagioli, C., Malgaroli, A., Pinton, P., Ripamonti, M., Rizzuto, R. and Sitia, R. (2012). Ero1α regulates Ca(2+) fluxes at the endoplasmic reticulum-mitochondria interface (MAM). *Antioxid. Redox Signal.* **16**, 1077-1087.

Cenci, S., Mezghrani, A., Cascio, P., Bianchi, G., Cerruti, F., Fra, A., Lelouard, H., Masciarelli, S., Mattioli, L., Oliva, L. et al. (2006). Progressively impaired proteasomal capacity during terminal plasma cell differentiation. *EMBO J.* **25**, 1104-1113.

Cortini, M. and Sitia, R. (2010). ERp44 and ERGIC-53 synergize in coupling efficiency and fidelity of IgM polymerization and secretion. *Traffic* **11**, 651-659.

Di Blasio, A. M., Centinaio, G., Carniti, C., Somigliana, E., Viganò, P. and Vignali, M. (1995). Basic fibroblast growth factor messenger ribonucleic acid levels in eutopic and ectopic human endometrial stromal cells as assessed by competitive polymerase chain reaction amplification. *Mol. Cell. Endocrinol.* **115**, 169-175.

Fraldi, A., Zito, E., Annunziata, F., Lombardi, A., Cozzolino, M., Monti, M., Spampanato, C., Ballabio, A., Pucci, P., Sitia, R. et al. (2008). Multistep, sequential control of the trafficking and function of the multiple sulfatase deficiency gene product, SUMF1 by PDI, ERGIC-53 and ERp44. *Hum. Mol. Genet.* **17**, 2610-2621.

Hamby, S. E. and Hirst, J. D. (2008). Prediction of glycosylation sites using random forests. *BMC Bioinformatics* **9**, 500.

Holbrook, L. M., Watkins, N. A., Simmonds, A. D., Jones, C. I., Ouwehand, W. H. and Gibbins, J. M. (2010). Platelets release novel thiol isomerase enzymes which are recruited to the cell surface following activation. *Br. J. Haematol.* **148**, 627-637.

Kakihana, T., Araki, K., Vavassori, S., Iemura, S., Cortini, M., Fagioli, C., Natsume, T., Sitia, R. and Nagata, K. (2013). Dynamic regulation of Ero1α and peroxiredoxin 4 localization in the secretory pathway. *J. Biol. Chem.* **288**, 29586-29594.

Lippincott-Schwartz, J., Yuan, L. C., Bonifacino, J. S. and Klausner, R. D. (1989). Rapid redistribution of Golgi proteins into the ER in cells treated with brefeldin A: evidence for membrane cycling from Golgi to ER. *Cell* **56**, 801-813.

Maeda, Y., Ide, T., Koike, M., Uchiyama, Y. and Kinoshita, T. (2008). GPHR is a novel anion channel critical for acidification and functions of the Golgi apparatus. *Nat. Cell Biol.* **10**, 1135-1145.

Masui, S., Vavassori, S., Fagioli, C., Sitia, R. and Inaba, K. (2011). Molecular bases of cyclic and specific disulfide interchange between human ERO1alpha protein and protein-disulfide isomerase (PDI). *J. Biol. Chem.* **286**, 16261-16271.

Mattioli, L., Anelli, T., Fagioli, C., Tacchetti, C., Sitia, R. and Valetti, C. (2006). ER storage diseases: a role for ERGIC-53 in controlling the formation and shape of Russell bodies. *J. Cell Sci.* **119**, 2532-2541.

Otsu, M., Bertoli, G., Fagioli, C., Guerini-Rocco, E., Nerini-Molteni, S., Ruffato, E. and Sitia, R. (2006). Dynamic retention of Ero1alpha and Ero1β in the endoplasmic reticulum by interactions with PDI and ERp44. *Antioxid. Redox Signal.* **8**, 274-282.

Pagani, M., Pilati, S., Bertoli, G., Valsasina, B. and Sitia, R. (2001). The C-terminal domain of yeast Ero1p mediates membrane localization and is essential for function. *FEBS Lett.* **508**, 117-120.

Qiang, L., Wang, H. and Farmer, S. R. (2007). Adiponectin secretion is regulated by SIRT1 and the endoplasmic reticulum oxidoreductase Ero1-L alpha. *Mol. Cell. Biol.* **27**, 4698-4707.

Ronzoni, R., Anelli, T., Brunati, M., Cortini, M., Fagioli, C. and Sitia, R. (2010). Pathogenesis of ER storage disorders: modulating Russell body biogenesis by altering proximal and distal quality control. *Traffic* **11**, 947-957.

Steentoft, C., Vakhrushev, S. Y., Joshi, H. J., Kong, Y., Vester-Christensen, M. B., Schjoldager, K. T.-G., Lavrsen, K., Dabelsteen, S., Pedersen, N. B., Marcos-Silva, L. et al. (2013). Precision mapping of the human O-GalNAc glycoproteome through SimpleCell technology. *EMBO J.* **32**, 1478-1488.

Swiatkowska, M., Padula, G., Michalec, L., Stasiak, M., Skurzynski, S. and Cierniewski, C. S. (2010). Ero1alpha is expressed on blood platelets in association with protein-disulfide isomerase and contributes to redox-controlled remodeling of alphaIIbbeta3. *J. Biol. Chem.* **285**, 29874-29883.

Vavassori, S., Cortini, M., Masui, S., Sannino, S., Anelli, T., Caserta, I. R., Fagioli, C., Mossuto, M. F., Fornili, A., van Anken, E. et al. (2013). A pH-regulated quality control cycle for surveillance of secretory protein assembly. *Mol. Cell* **50**, 783-792.

Wang, L., Wang, L., Vavassori, S., Li, S., Ke, H., Anelli, T., Degano, M., Ronzoni, R., Sitia, R., Sun, F. et al. (2008). Crystal structure of human ERp44 shows a dynamic functional modulation by its carboxy-terminal tail. *EMBO Rep.* **9**, 642-647.

Wang, Z. V., Schraw, T. D., Kim, J. Y., Khan, T., Rajala, M. W., Follenzi, A. and Scherer, P. E. (2007). Secretion of the adipocyte-specific secretory protein adiponectin critically depends on thiol-mediated protein retention. *Mol. Cell Biol.* **27**, 3716-3731.

Wilson, D. W., Lewis, M. J. and Pelham, H. R. B. (1993). pH-dependent binding of KDEL to its receptor in vitro. *J. Biol. Chem.* **268**, 7465-7468.

Zito, E., Buono, M., Pepe, S., Settembre, C., Annunziata, I., Surace, E. M., Dierks, T., Monti, M., Cozzolino, M., Pucci, P. et al. (2007). Sulfatase modifying factor 1 trafficking through the cells: from endoplasmic reticulum to the endoplasmic reticulum. *EMBO J.* **26**, 2443-2453.